

Measurement of sensitivity of solar blind UV cameras to solar light

K. Chrzanowski^{a,b}  and B. Stafiej^b

^a Military University of Technology, Institute of Optoelectronics, 2 gen. Kaliskiego St., 00-908 Warsaw, Poland

^b INFRAMET, Bugaj 29a, Koczargi Nowe, 05-082 Stare Babice, Poland

Article info

Article history:

Received 26 Mar. 2021

Received in revised form 20 May 2021

Accepted 21 May 2021

Keywords:

Solar sensitivity, SBUV cameras, solar blind UV cameras, UV cameras sensitivity, corona discharge detection.

Abstract

Solar blind UV cameras are not theoretically supposed to be sensitive to solar light. However, there is practically always some sensitivity to solar light. This limited solar sensitivity can sometimes make it impossible to detect the weak emission of a corona target located on the solar background. Therefore, solar sensitivity is one of the crucial performance parameters of solar blind UV cameras. However, despite its importance, the problem of determining solar sensitivity of solar blind UV cameras has not been analysed and solved in the specialized literature, so far. This paper presents the concept (definition, measurement method, test equipment, interpretation of results) of measuring solar sensitivity of solar blind UV cameras.

1. Introduction

Solar blind ultra-violet (SBUV) cameras are cameras sensitive to a UV light below about 280 nm where, due to the absorption by the Earth's atmosphere ozone layer, there is almost no sunlight. SBUV cameras are theoretically insensitive to solar light. However, in practice there is always some sensitivity to solar light. This can sometimes make it impossible to detect the weak emission of a corona target located on the solar background. Therefore, solar sensitivity should be treated as one of the crucial performance parameters of SBUV cameras. However, despite its obvious importance, this parameter is not presented in data sheets of typical SBUV cameras [1-6]. More importantly, the available scientific papers devoted to the characteristics of SBUV cameras did not present any concept on how to measure this parameter [7-11]. In such a situation this paper presents the concept (definition, measurement method, test equipment, interpretation of results) of measuring solar sensitivity of SBUV cameras. This new concept is expected to help precisely characterize the ability of SBUV cameras operating under ultra-bright daylight conditions.

2. Task of SBUV cameras

Great majority of SBUV cameras are used for detection of corona discharges from high-voltage power lines. Therefore, this paper focuses on testing SBUV cameras for corona detection. The task of such cameras is to detect a weak emission of UV light from small size elements of high-voltage power lines. Due to their size, the targets of interest fill only small parts of camera FOV (Fig. 1). If tests are performed on a bright day, the background may scatter/reflect some light originally emitted by the Sun that reaches a SBUV camera.

Power lines maintenance tests are typically done by ground crews using an SBUV camera looking up at power lines against the sky. In this case, the sky (thick layer of air behind the targets) emits solar light due to a scattering effect. If a signal generated by the sky is comparable to or higher than a signal generated by the corona target, then the corona target will not be detected. The angle between the optical axis of a SBUV camera used by ground crews and the horizontal plane can vary from near 0° to about 90°. However, it is typically in the range of 20° to 60°.

Tests using helicopters or drones as platforms for SBUV cameras are the second increasingly popular way for high-voltage power lines maintenance tests. In this case,

*Corresponding author at: kch@inframet.pl

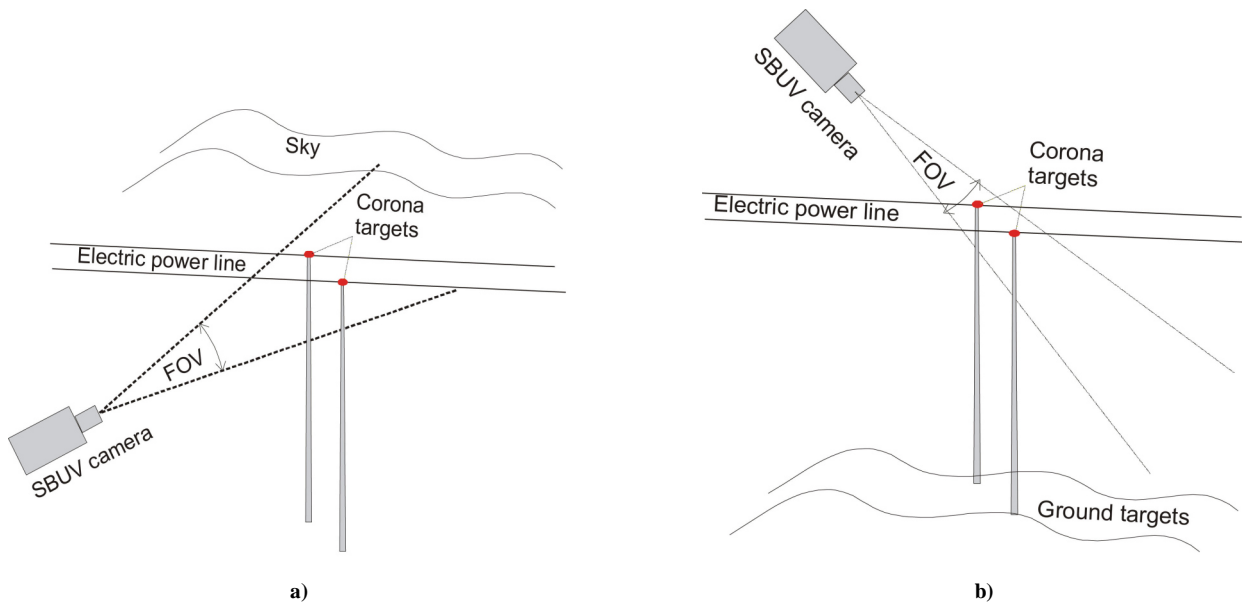


Fig. 1. Two types of backgrounds of corona targets a) sky background, b)ground background

the SBUV camera looks down at natural/artificial ground objects that form the background of the target of interest. The SBUV camera receives light emitted by the Sun that is reflected by the ground. The angle between the optical axis of an airborne SBUV camera and the horizontal plane can vary significantly from 10° to 90°.

3. Reasons for SBUV cameras sensitivity to solar light

From the construction point of view, SBUV cameras can be treated as intensified CMOS (ICMOS) cameras with a spectral band limited by a set of filters to the so-called SBUV band (from about 240 nm to about 280 nm) coupled with a typical CMOS camera working in the visible band.

Numerous scientific papers report that there is practically no sunlight at wavelengths below 280 nm due to a very high absorption by the ozone layer of the Earth’s atmosphere [12,13]. Therefore, an SBUV camera equipped

with a perfect solar blind filter (transmittance equal to one at wavelengths below 280 nm and equal to zero at wavelengths over 280 nm) will not be sensitive to solar radiation. However, it is not technically possible to manufacture such a perfect edge solar blind filter. There is always a narrow band where the filter transmission changes from high to very low. Therefore, a relative spectral sensitivity function of typical SBUV cameras resembles the Gauss function of a centre at 260 nm that can partially overlap with a relative spectral total solar light intensity (Fig. 2). Data on the relative sensitivity of cameras should be treated as the author’s estimation based on a structural analysis of SBUV cameras. Data on the relative total solar light intensity is taken from Ref. 14 as the relative hemispherical spectral solar irradiance.

It should be also noted that real SBUV filters often have some leakage at visible and near infrared spectral bands. Therefore, the background emitting high intensity light in the VIS/NIR spectral band can potentially generate a signal detectable to SBUV cameras.

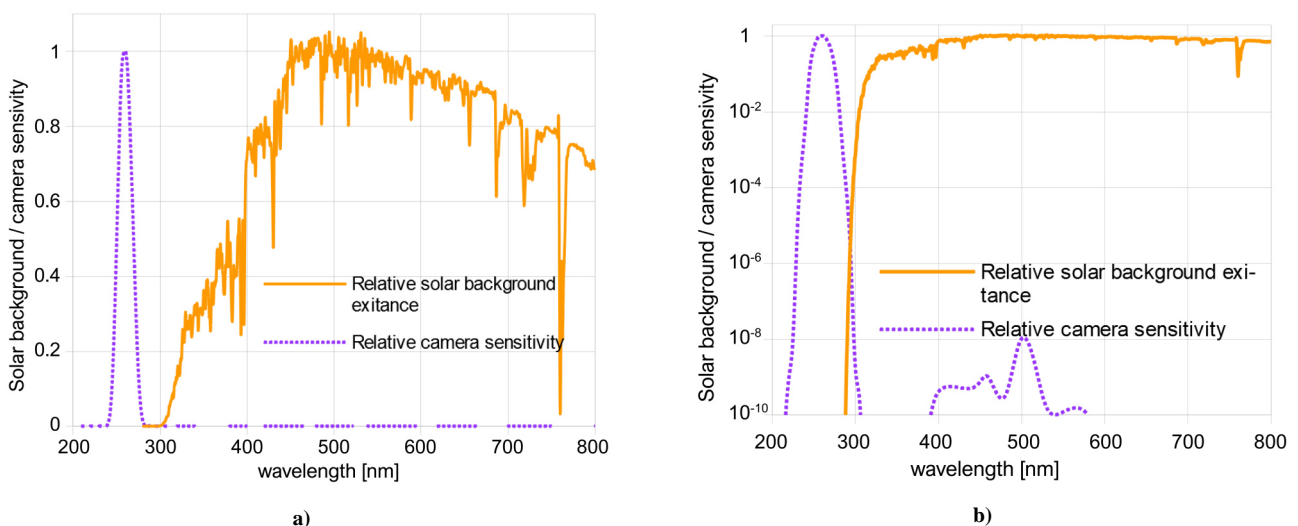


Fig. 2. Relative SBUV camera sensitivity $s(\lambda)$ and relative total solar light intensity: a) linear scale, b) logarithmic scale

4. Characterization of the background of corona targets

Sky is the name of the Earth's atmosphere and outer space as seen from the ground level. Ground targets are irradiated directly by the Sun and indirectly by the diffusive light emitted by the Sun and scattered by the atmosphere of the hemispherical sky firmament. Since only a very small part of the sky emits/transmits a direct solar light, the term 'sky' will be limited to the part emitting a scattered solar light.

Ground background is a term that refers to a long series of natural/artificial land or water objects that can be in FOV of airborne SBUV cameras. This type of the background does not emit its own light. It reflects incoming solar light (Fig. 3).

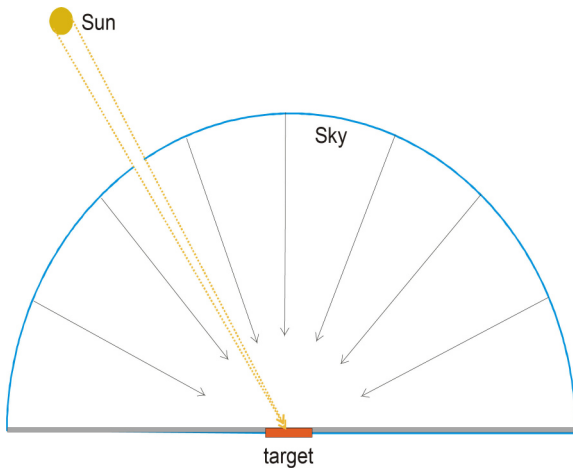


Fig. 3. Two components of light that illuminate ground targets: 1) direct Sun light, 2) diffusive sky light.

Both sky and ground can be considered as the area light sources and their light intensity can be characterized using a quantity called radiance L expressed in $W/(sr \cdot m^2)$ unit.

If we assume that the sky is a uniform Lambertian light source, then the radiance L_{sky} of the sky background can be calculated as:

$$L_{sky}(\lambda) = M_{sky}(\lambda)/\pi \approx E_{sky}(\lambda)/\pi, \quad (1)$$

where M_{sky} is the radiant exitance of the sky and E_{sky} is the irradiance of the horizontal target due to a diffusive light emitted by the sky firmament.

More specifically, the assumption that the sky is a Lambertian light source is reasonable because of the scattering of solar light by the sky atmosphere. However, assuming the sky uniformity is more risky. The sky firmament is never fully uniform and the radiance of light emitted by the sky often depends on the observation angle [15]. Moreover, the non-uniformity level depends on date and time. Therefore, Eq. (1) refers to the average sky radiance.

If we assume that the diffusive reflectance of the ground target is much higher over its specular reflectance, then the radiance of the ground background L_{ground} can be calculated as follows:

$$L_{ground}(\lambda) = \rho(\lambda) (E_{sun}(\lambda) + E_{sky}(\lambda))/\pi, \quad (2)$$

where $\rho(\lambda)$ is the diffusive spectral reflectance of the ground background, E_{sun} is the irradiance of the horizontal target due to a direct solar light emitted by the Sun.

Equations (1) and (2) show clearly that it is possible to calculate radiance of both the sky and the ground background if spectral irradiance and spectral reflectance of the simulated target are known. The problem is that spectral irradiance due to the direct solar light, spectral irradiance due to the diffusive sky light, and spectral reflectance of the ground targets depend on a series of factors. For irradiance due to the direct solar light and irradiance due to the light emitted by the sky, these are: latitude, longitude, altitude, date, time, pressure, temperature, relative humidity, ozone, precipitable water, industrial pollution level [12,13]. Spectral reflectance of the ground targets varies a lot, depending on a type of a natural/artificial material used to create a surface of such targets [16].

In such a situation, it is clear that some reference average solar lighting conditions supported by international standards would be useful for a characterization of SBUV cameras.

Photovoltaic cells have become an important green source of energy that generates electric power when illuminated by solar light. The Sun emits great majority of its light in the spectral range from 280 nm to about 2500 nm. This fact has generated a great interest in properties of the solar light illuminating ground level targets and led to a creation of an internationally recognized standard (ASTM G173) that presents the spectral irradiance of a flat target located on the Earth's ground at simulated average reference conditions [14]. In detail, the standard presents the spectral irradiance of the reference target tilted at 37° (target receives a mix of light from the sky and the ground) caused by light coming directly from the Sun (including circumsolar light) or the total hemispherical irradiance caused by a sum of direct solar light and diffusive sky light.

The standard is of limited use for testing the solar sensitivity of SBUV cameras because it does not present the spectral irradiance of diffusive sky background and spectral reflectance of ground targets required by Eqs. (1) and (2).

However, there is a publicly available computer program SMARTS that was used to calculate spectral data presented in the ASTM G173 standard [17-19]. The input settings of this program can be modified to generate output data needed by Eqs. (1) and (2):

1. Spectral irradiance E_{sky} of a horizontal target irradiated by diffusive light emitted by the sky background,
2. Spectral irradiance E_{ground} of a horizontal target irradiated by the direct solar light,
3. Spectral reflectance $\rho(\lambda)$ of a series of ground objects.

However, there is still a question for what conditions the irradiance E_{sky} , and irradiance E_{sun} , are to be calculated and what material is to be chosen for a ground target surface.

As has been mentioned above, the irradiances E_{sky} and E_{sun} depend on a long series of parameters: latitude, longitude, altitude, date, time, pressure, temperature, relative humidity, ozone, precipitable water, and industrial pollution level. However, the first five of these parameters (latitude, longitude, altitude, date, time) actually describe the Sun elevation relative to the horizontal ground plane. The rest of these parameters (pressure, temperature, relative humidity, ozone, precipitable water, and industrial pollution level) are meteorological conditions that can be roughly characterized by a geographical region indication.

Ozone is the most important UV absorbent. Distribution of ozone varies depending on the geographical location (Fig. 4). The higher the concentration, the less amount of solar UV will reach the camera. This is beneficial for the users. However, a camera calibrated for the high ozone sky may have insufficient attenuation when operated in low ozone regions. SMARTS allows to change the ozone concentration in its simulations. A comparison of solar spectra of different ozone concentration is shown in Fig. 5. ASTM G173 uses approximately 343DU in its calculation.

The world can be roughly divided into ten regions of atmosphere (US Standard, MLS – Mid-Latitude Summer, MLW – Mid-Latitude Winter, SAS – Subarctic Summer, SAW – Subarctic Winter, TRL – Tropical, STS – Subtropical Summer, STW – Subtropical Winter, AS – Arctic Summer), AW - Arctic Winter) on the basis of the criterion of typical meteorological conditions [21]. The difference

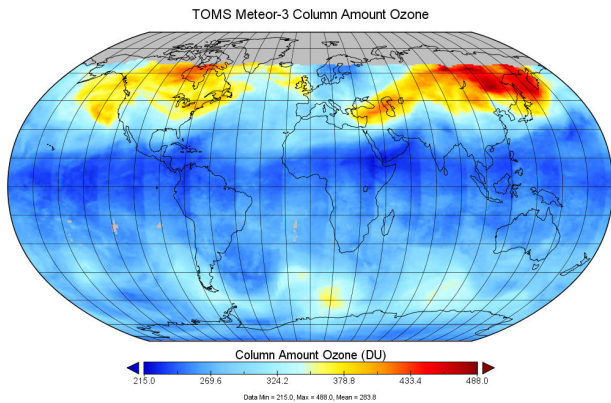


Fig. 4. Ozone concentration distribution [20].

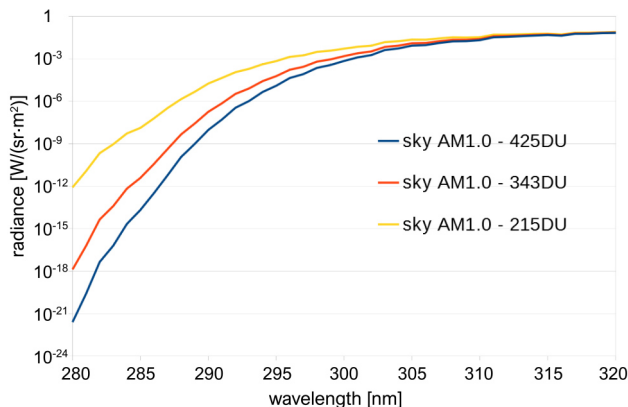


Fig. 5. Impact of ozone concentration on sky spectrum in UV region.

between US Standard and MLS atmosphere is minimal. Since the concentration of ozone is seasonal [22], there is a noticeable difference in summer and winter climate variants. The calculated sky irradiance in the UV region for MLS and MLW climates assuming the same AM coefficient is shown in Fig. 6.

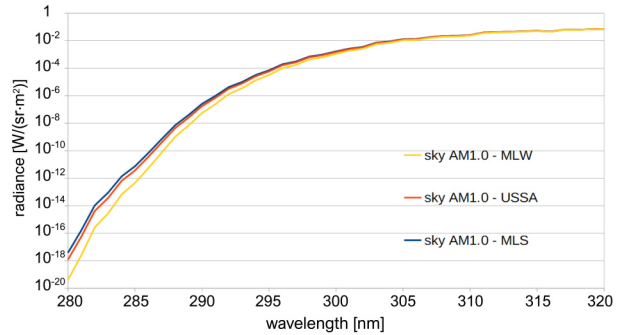


Fig. 6. Comparison between MLS and MLW climates for AM1.0 sky radiance.

The elevation angle of the Sun determines the apparent relative thickness of the atmosphere layer for a direct solar light. This relative thickness of the atmosphere is called the Air Mass (AM) coefficient. It is commonly considered as the most important parameter to describe the Earth's surface illumination by solar light [23].

It should be noted that the AM coefficient depends on the Sun elevation angle and can be calculated using Eq. (3) [24]:

$$AM = \frac{L}{L_0} \approx \frac{1}{\cos(z)} = \frac{1}{\cos(90^\circ - \alpha)}, \quad (3)$$

where L is the path length of a direct solar light through the atmosphere at the specified zenith angle z . L_0 is the same path length but for the zenith angle $z = 0^\circ$. Equation can be converted including the elevation angle α that equals 90° minus z .

ASTM G173 standard presents reference illumination spectra only for AM1.5 coefficient and for US Standard Atmosphere [16]. This AM coefficient value refers to illumination conditions when the Sun elevation is about 52° in the southwest states of the USA [19]. In less accurate terms, it can be said that the ASTM G173 standard describes the average illumination condition for the industrialized northern hemisphere belt: USA, Europe, China.

Situation for testing solar blind SBUV cameras is different. Tests under average conditions are not enough. SBUV cameras should work any date, any time, and in all geographical locations. Thus, let us assume the worst-case scenario for SBUV cameras: working during the day and at the time when the Sun is at its highest elevation in local conditions.

The world is divided into ten geographical zones: Equatorial: $10^\circ N - 10^\circ S$, Tropical: $10^\circ N - 25^\circ N$ and $10^\circ S - 25^\circ S$, Subtropical: $25^\circ N - 35^\circ N$ and $25^\circ S - 35^\circ S$, Mid-Latitude: $35^\circ N - 55^\circ N$ and $35^\circ S - 55^\circ S$, Subarctic: $55^\circ N - 60^\circ N$, Subantarctic: $55^\circ S - 60^\circ S$, Arctic: $60^\circ N - 75^\circ N$, Antarctic: $60^\circ S - 75^\circ S$, North Polar: $75^\circ N - 90^\circ N$, South Polar: $75^\circ S - 90^\circ S$ [25]. Nevertheless, the latter four zones are practically not inhabited and can be excluded from the analysis.

There are always at least two days per year when the Sun elevation equals 90° for locations in the belt between Tropic of Cancer and Tropic of Capricorn (up to about $\pm 23^\circ$ latitude – approximately equatorial and tropical zones). The maximum elevation angle of the Sun in other geographical zones is not as high. In most of the northern hemisphere (Subtropical, Mid-Latitude, Subarctic, Arctic zones) the maximum Sun elevation occurs on about June 21st, and the minimum elevation occurs on about December 21st [26]. The opposite situation is in the southern hemisphere.

It is commonly known that the average illumination intensity varies very significantly (at least 4 times) depending on the latitude of the location of interest [27]. However, the data shown in Table 1 calculated using a publicly available solar position calculator [26] suggest surprising conclusions that for locations in inhabited areas (Arctic/Antarctic excluded) variations of the maximum elevation angle are much smaller (from about 50° to 90°). What is even more important is that the variation of the minimum AM coefficient in geographical locations in typical inhabited geographical zones is small. It can be seen that the AM coefficient of geographical locations in inhabited zones (Arctic/Antarctic excluded) varies in the narrow range from 1 to about 1.25. If Subarctic/Subantarctic zone is excluded, then the AM coefficient will differ only in the range from 1 to about 1.15.

The explanation for this very low dependence of the maximum AM coefficient on the elevation angle is the non-linear dependence of AM on the Sun elevation angle as shown in Eq. (3).

The practical implications of the data presented in Table 1 are that if tests of SBUV cameras are to be done for the worst-case scenario, then they should be carried out for illumination conditions when the AM coefficient is close to

one (AM1.0), regardless of the geographical zone they are intended to be used.

It should be remembered that the SBUV cameras working in equatorial/tropical zones will meet extremely high illumination conditions almost every day when the SBUV cameras working in the subarctic zone can meet the similar illumination conditions only during a short summer. If the summer is rainy/cloudy, then these extreme illumination conditions are never to be met. Therefore, it could be reasonable to carry out additional tests of solar blindness of SBUV cameras for the sky background of spectral radiance calculated for AM1.5 air mass. These conditions could be treated as mild extreme for cameras working in subarctic zone or as average conditions for cameras working in mid-latitude zone.

As discussed earlier, the solar illumination depends on a geographical zone (type of atmosphere). It means that the spectral irradiance for the same AM coefficient will be different for different zones [21]. However, the difference between spectral irradiances obtained for most inhabited areas in the northern hemisphere in the summer time (atmosphere: US Standard, MLS, SAS) is minimal compared to the change of AM from 1.1 to 1.5. Therefore, further calculations will be done for US Standard atmosphere because this atmosphere can be considered as typical for the world industrialized belt of USA-Europe-China.

Determination of the AM coefficient and the atmosphere type is enough to determine input settings for SMARTS computer program [21] to generate input data (spectral irradiance of a horizontal target due to irradiance by the sky firmament diffusive light) that can be used to calculate spectral radiance of the sky background of corona targets. Figure 7 shows the results for two simulated conditions. (AM1.0 and AM1.5).

Table 1.

Approximate latitude, elevation angle, and AM coefficient for a series of world cities located in different geographical zones.

City	Caracas	Cairo	Washington	Beijing, China	Berlin	Moscow	Helsinki
Zone	Tropical	Subtropical	Mid-Latitude	Mid-Latitude	Mid-Latitude	Subarctic	Subarctic
Latitude	10.5	30.04	38.9	39.9	52.5	55.7	60.2
Max. elevation	90	80.52	74.37	73.15	61.07	57.14	53.04
Min. elevation	55	35.94	27.73	26.63	14.19	10.69	6.47
Min. AM	1.00	1.01	1.04	1.04	1.14	1.19	1.25
Max. AM	1.22	1.70	2.15	2.23	4.08	5.39	8.87

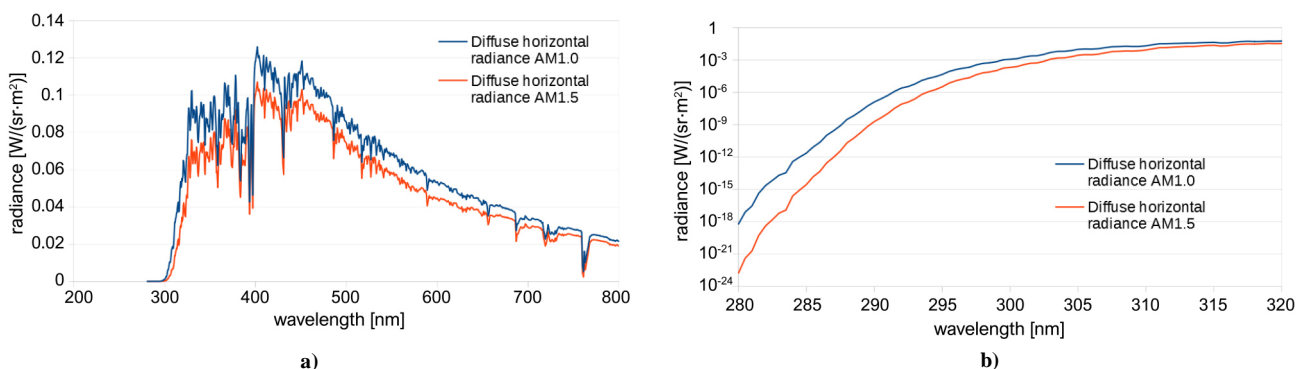


Fig. 7. Radiance of the sky for two simulated AM coefficients: a) linear scale, b) logarithmic scale.

Analysis of data presented in Fig. 7 shows that the maximum of light intensity is in a band from about 350 nm to about 500 nm. Next, the difference between spectral radiance for AM1.0 and AM1.5 is generally minimal, but there is a noticeable wavelength shift at a 280–300 nm band that can generate a significant difference in solar sensitivity of the SBUV cameras.

There are dozens of materials that can create natural/artificial targets surface that forms a ground background for the SBUV cameras:

1. Soils (bare soil, dry clay soil, wet clay soil, black loam, light clay, light loam, pale loam, dry soil, light soil, brown loam, wet sandy soil, wet red clay, wet silt);
2. Sands (dry sand, white sands, brown sand, dune sand, dark sand);
3. Water (calm ocean, seawater, open ocean seawater, coastal seawater);
4. Snow (fresh dry snow, snow on a mountain, névé, melting snow, solid ice, granular snow, fresh fine snow);
5. Trees (pinyon pine tree, fir trees, Norway spruce tree, ponderosa pine tree, conifer trees, deciduous trees, birch leaves, deciduous oak tree leaves, grazing field);
6. Rocks (basalt rock, granite);
7. Fields/meadows (dry grass, green rye grass, green grass, perennial rye grass, alpine meadow, lush meadow, dry long grass, lawn grass, field crops - wheat crop, tall green corn);
8. Artificial construction materials (concrete slab, old runway concrete, old runway asphalt, terracotta roofing clay tile, red construction brick, plywood sheet, white vinyl plastic sheet, clear fibreglass greenhouse roofing, galvanized corrugated sheet metal).

Spectral reflectance data for the full spectral range from about 300 nm to 800 nm are available only for the material fractions listed above [21]. However, even a quick analysis of such data can lead to the conclusion that for most of the analysed materials the UV reflectance is low (below 0.1) and gradually increases with the wavelength in the VIS-NIR range. Next, it looks like the average reflectance of artificial materials is generally higher compared to that of natural materials. Subsequently, concrete slabs represent the material with the highest spectral reflectance among the common materials used in buildings or road constructions that can be commonly found as ground backgrounds of

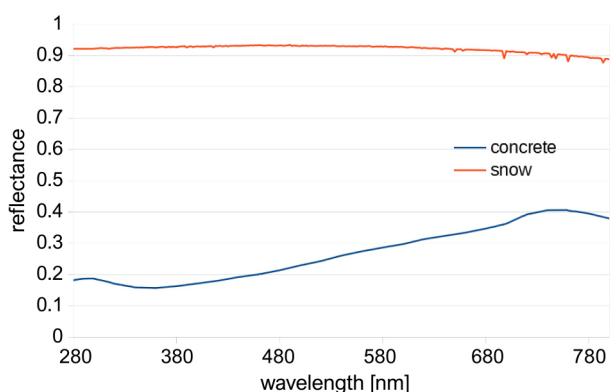


Fig. 8. Spectral reflectance of concrete slabs and of fresh, dry snow.

SBUV cameras (Fig. 8). Therefore, a concrete slab will be chosen as one of the reference ground backgrounds.

Snow is an exception among natural materials that can potentially form a ground background of SBUV cameras due to its uniform, very high reflectance in the range from deep UV to NIR (Fig. 8). Snow background can be rarely found in the late spring/early summer when the Sun is at its highest elevation and the AM coefficient equals one. Hence, let us assume that the snow background can occur only at a period when the AM coefficient (related to the Sun elevation) is not lower than 1.5. Spectral radiance of these three extreme types of background of SBUV cameras is presented in Fig. 9.

5. Field tests of solar sensitivity

SBUV cameras are designed for use in the field to detect corona targets having backgrounds illuminated by solar light. Thus, tests of SBUV cameras sensitivity to solar light done under field conditions look logical and apparently easy. However, practically measuring solar sensitivity under field conditions is not so easy, and results can be confusing.

It can be logically expected that both manufacturers and users of SBUV cameras do some practical verification of solar blindness of SBUV cameras under field conditions, but it is not clear what are details of these tests due to the lack of publicly available information. However, based on non-formal communication channels, the authors know that the tests of SBUV cameras solar blindness commonly performed in the field can be divided into three groups:

1. analysis of images of corona targets captured at a series of possible work scenarios,
2. analysis of the Sun image,
3. analysis of the sky background image.

All three methods look apparent as claimed, but have some limitations.

The first method can potentially deliver precise information on the SBUV cameras solar sensitivity. The problem is that this method requires very long series of SBUV camera testing experiments at different times of year, time of day, geographical location, meteorological conditions, corona target types, and background times to obtain reliable results valid for great majority of possible work scenarios. Due to the high costs and very long time, this method cannot be practically applied, or at least for full-scale tests.

The second method seems to be an easy solution that can generate clear results that can be taken as a worst-case scenario. It is easy to point the tested SBUV camera towards the Sun and check what the output image looks like. The test teams expect that a so-called “good” SBUV camera will not generate a detectable image of the Sun, or at least the image will be barely detectable compared to internal noise. The “bad” SBUV cameras are expected to generate a detectable image of the Sun. It is correct that this method is easy to use and offers clear results in a very short time. However, the results can be confusing despite the method simplicity and apparent error proof.

First, it should be noted that the direct Sun method assumes that the Sun fills part of the camera FOV. In reality, such conditions are never to be met in real work. The Sun is never in camera FOV in real work to prevent saturation of the visible channel of the SBUV camera.

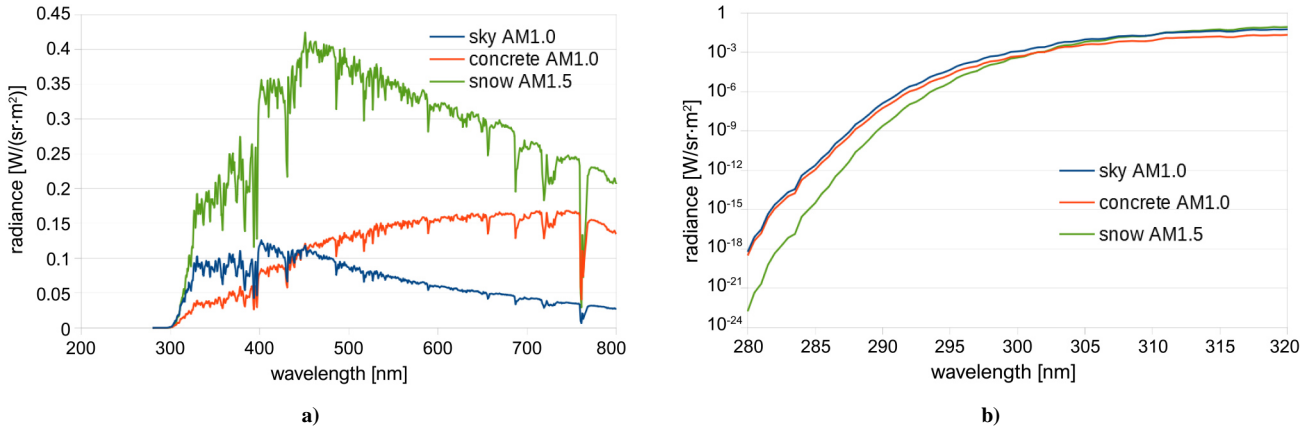


Fig. 9. Spectral radiance of three extreme solar backgrounds: a) linear scale, b) logarithmic scale.

Second, the direct Sun method is based on the assumption that the Sun can be treated as a light source with spectral radiance that is similar but always higher than spectral radiance of the corona targets solar backgrounds in real work scenarios. The problem is that this assumption is not always fulfilled. In order to prove this claim, let us calculate the Sun radiance on the basis of available irradiance data.

It is commonly presented in educational books that the angular size of the Sun is about 0.5°. However, the apparent angular size of the Sun disk, that emits light directly illuminating ground targets, is several times bigger: $\Omega = 2.5^\circ = 0.006 \text{ sr}$ [28]. For simplicity, both the light emitted by Sun and the light emitted by a circumsolar will be treated as direct solar light and it should be assumed that the solar disk radiance is uniform. For such conditions, the relationship between the average radiance of the solar disk L_{sun} and the direct solar irradiance E_{sun} is:

$$L_{sun}(\lambda) = E_{sun}(\lambda) / \Omega \approx 166.7 E_{sun}(\lambda), \quad (4)$$

where Ω is the solid angle subtended by the Sun disk seen by the observer positioned as Earth.

The sky background at AM1.0 conditions can be considered as possible highest limit of the corona targets sky background. It can also be easily agreed that majority of the Sun direct tests is done by users in the mid-latitude geographical zone of the Sun at an altitude equivalent to the

AM not lower than 1.5. Therefore, let us compare the radiance of the Sun at AM1.5 and the radiance of the sky at AM1.0.

Results of the calculations of the Sun radiance at AM1.5 using Eq. (4) and the sky radiance at AM1.0 using Eq. (1) are shown in Fig. 10. These results show that:

1. Average spectral radiance of the Sun disk at AM1.5 is about one thousand times higher compared to the average spectral radiance of the sky firmament at AM1.0 in a spectral band from about 300 nm to about 800 nm [Fig. 10a].
2. Spectral radiance of the sky firmament at AM1.0 is higher than the spectral radiance of the Sun disk at AM1.5 in a spectral band from 280 nm to about 290 nm [Fig. 10b].

These two conclusions proved that the Sun is a wrong target to test solar sensitivity of SBUV cameras because it favours cameras designed in a wrong way. In detail, this method requirements are too relaxed in the 280–290 nm spectral band, but are unreasonably high in the 400–800 nm band.

It is much more reasonable to do tests of solar blindness of SBUV cameras by field tests against the sky firmament emitting diffuse light that fills the camera FOV. Such tests are often done, as well. However, sky radiance depends on a series of input parameters: geographical position, annual time, day time, meteorological conditions, industrial pollution level, and angle of observation.

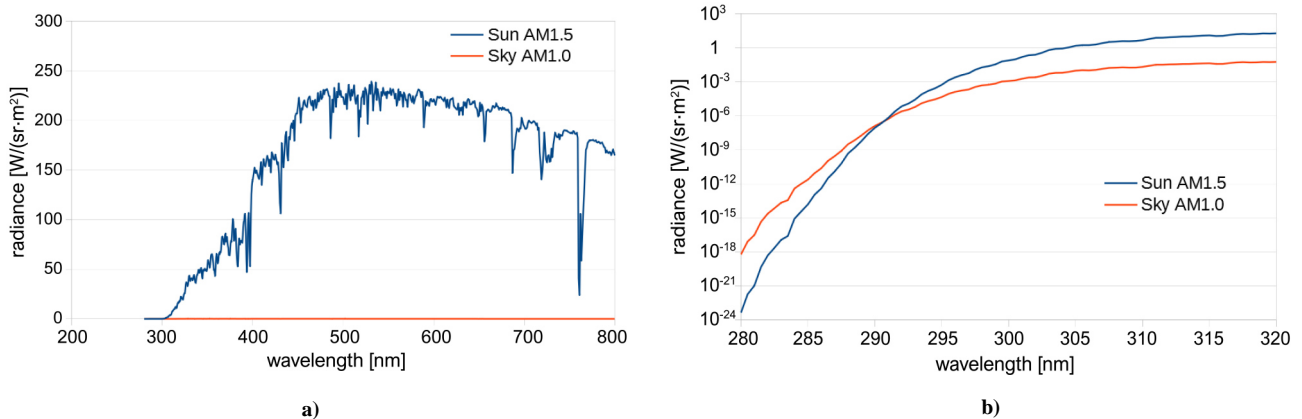


Fig. 10. Spectral radiance of the Sun disk at AM1.5 and spectral radiance of the sky firmament at AM1.0: a) linear scale, b) logarithmic scale.

Field tests in areas close to industrial sites are particularly risky for two reasons. First, ozone increased density in the air is often recorded in such areas and this effect leads to an attenuation increase of solar light at the 280–310 nm spectral band. Second, welding outside buildings can create a noticeable increase in both UV and visible light scattered by the atmosphere. All these factors create a situation when field tests results are not only geographically and time-dependent, but can differ even if repeated in the same place and time. Thus, field tests are limited to accurately evaluate solar sensitivity of SBUV cameras.

6. Concept of laboratory solar tests

The conclusions from the previous section clearly showed that a test system offering repeatable reliable tests of solar blindness of SBUV cameras in laboratory conditions, simulating some reference solar backgrounds, is needed. If we assume that the test system is to simulate most extreme cases that can be met in real work of SBUV cameras, then a simulation of at least three cases is needed:

1. Sky background in the summer time at a very high elevation of the which corresponds to the AM1.0;
2. Concrete slab background in the summer time at a very high elevation of the Sun which corresponds to the AM1.0;
3. Snow background in the spring time at a moderate elevation of the Sun which corresponds to AM1.5.

It is highly probable that if an SBUV camera is not sensitive to any of these solar backgrounds, then the Sun illumination will not degrade work efficiency of such camera in any geographical location, date, time, meteorological conditions, or solar background type. It should be noted that the number of simulated solar backgrounds can be limited to the first two backgrounds for countries in geographical zones where the likelihood to encounter a spring snow background is near zero.

Now, let us explain how solar sensitivity can be measured. It is proposed to define solar sensitivity as the ratio of the output signal (spatio-temporal density of even counts) at the output of the SBUV camera generated by a reference solar background to the average output signal generated by the camera noise:

$$SolarS = \frac{S(L_{ref}(\lambda))}{S_{noise}}, \quad (5)$$

where L_{ref} is the radiance of the reference solar background, $S(L_{ref})$ is the output signal due to the reference background light, S_{noise} is the output signal due to the internal camera noise (radiance of simulated background equal to zero).

Please note that there are different reference solar backgrounds and the type of simulated background should be specified in the results of the measured solar sensitivity.

The task of testing sensitivity of SBUV cameras to solar light using an artificial solar simulator also looks easy because there are many solar simulators offered on the international market (Solar Light Company, Atonometrics, Eternal Sun, TS-Space Systems, WACOM, Newport Oriel, Sciencetech, Spectrolab, Photo Emission Tech, Abet Technologies, InfinityPV, and many others). All these companies offer solar simulators based on a variable intensity and a variable spectrum light source in the spectral

range from UV to NIR. Next, there is a very numerous literature on solar simulators. Only SPIE digital library offers hundreds of scientific papers devoted to solar simulations. In addition, there is also a series of standards presenting detail requirements for solar simulators (IEC 60904-9, ASTM E927-10, ISO 24444:2010). However, all these commercially available solar simulators, scientific papers, and standards devoted to solar simulation introduce a limited or very limited usefulness for testing SBUV cameras due to several reasons.

First, typical solar simulators are designed to simulate irradiation of a target of interest by solar light emitted by the Sun, sky, clouds, land, or sea. The device under test (typically a photovoltaic solar panel) is to be inserted to the target plane of the solar simulator. When testing SBUV cameras, we do not need to know the irradiance in the camera optics plane, but the radiance (or radiant exitance) of solar backgrounds (sky, clouds, land, or sea). Therefore, we cannot just insert a tested SBUV camera into a typical solar simulator and run solar sensitivity tests. A light source is needed that can emit light of a spectral radiant exitance/radiance resembling the spectral radiant exitance/radiance of sky, clouds, ground targets, or mixed light emitted by all these targets when the camera under test looks at the solar simulator from a distance. Hence, it is necessary to redesign a typical solar simulator to convert it from irradiance standard to radiant exitance (radiance) standard.

Second, the spectral band from 280 nm to about 320 nm is outside the calibrated spectrum of almost all solar simulators since it is not interesting for typical applications like photovoltaic cell testing due to the extremely low flux in this band compared to the total flux in full spectrum. However, this spectral band is of critical importance when testing the influence of the solar background on the performance of SBUV cameras. It is due to a possible overlapping of the solar spectrum with the spectral sensitivity function of the tested camera (see Fig. 2).

Third, some solar simulators offer changes in the spectrum of the emitted light using so-called air mass filters [29], but they achieve the light spectrum similar to that of the total hemispherical light reaching the ground level and not similar to the simulated background.

Fourth, there are several solar simulators (called UV solar simulators) developed for the cosmetic industry to irradiate tested specimen with light with a calibrated spectrum from 250 nm to 800 nm [30]. Nevertheless, the irradiance level in the band of 250–320 nm is much too high to simulate solar backgrounds met when testing SBUV cameras. It is officially accepted in this type of UV solar simulators that the minimum measurable irradiance at 290 nm is 10^{-4} W/(nm·m²) [31] while some SBUV cameras are capable to detect light at this wavelength weaker by several sizes.

Fifth, a typical equipment capable of calibrating typical solar simulators is not sensitive enough to calibrate solar background simulators needed for testing SBUV cameras. It is officially stated by the top world national metrology laboratory that the spectral radiance of light sources in the spectral band from 220 nm to 2500 nm can be measured at a level not lower than $4 \cdot 10^{-3}$ W/(sr·nm·m²) [32]. Converting to the radiant exitance, we get the minimum measurable level at $12.56 \cdot 10^{-3}$ W/(nm·m²) in a situation when the SBUV

cameras are capable to detect corona sources of radiant exitance at the level of at least 10^{-10} W/(nm·m²).

To summarize, there is no commercially available solar simulators suitable to be used as background simulators for the solar tests of SBUV cameras and such simulators must be developed. The same can be said about the methods and equipment needed to calibrate solar background simulators. Thus, it is necessary to develop new technical solutions for the measurement of the SBUV cameras solar sensitivity.

7. Technical solution for a solar test station of SBUV cameras

Sensitivity (noise parameters) of cameras sensitive to the visible and near infrared light is measured using two methods based on the different design test systems (Fig. 11):

1. Tested camera is located at a very short distance from a large light source with adjustable light intensity that fills its Field Of View (FOV),
2. Tested camera is located at the collimator output that projects an image of a small light source located in its focal plane. Refractive or reflective collimators are used as image projectors.

There are logically no obstacles why not use the same approach to test SBUV cameras. However, SBUV cameras use optics of aperture as big as about 80 mm. Designing a light source of a big emitter capable to simulate a very bright solar background is a difficult task. The task can be easier in case of light sources of a smaller emitter. Therefore, let us choose the solution based of an image projector that could project images of simulated solar backgrounds shown in Fig. 11b). However, the general test concept is not enough. Precise design guidelines are needed.

The aim of the solar test station is to simulate the solar backgrounds of corona targets that can be met during real work of SBUV cameras. There can be myriads of such backgrounds. Even if we limit interest to worst-case scenarios, then we can have at least 3 different types of backgrounds (different average radiance and different spectrum). Therefore, an ideal test system should be able to project images of at least 3 types of solar backgrounds listed in section 4.

The solar test system is to be built from three main blocks: collimator, light source, image acquisition/analysis system.

The task of the collimator is to project the image of the light source emitter located in its focal plane. The light source is characterized by the same (or similar) spectral

radiance as the simulated solar background. Image acquisition/analysis system (PC, frame grabber, software) should enable capturing of the output images generated by the tested SBUV camera and calculation of the output signal (spatio-temporal density of event counts) of the light source image.

Angular size of the projected image of the light source should be large enough to be considered a large target to eliminate influence of the source size on the output signal. FOV of typical SBUV cameras differs in the range from about 3° to 10°. Therefore, it can be estimated that light source of the angular size of about 2° can be considered a large target for each SBUV camera. In the case of large targets, some deterioration of the projected image quality by the collimator is acceptable. Thus, any refractive or reflective optical collimator suitable for work in the spectral band from 280 nm to 800 nm can be used.

The light source is the critical and most difficult block of the solar test system to develop. The ideal light source working as a solar simulator should enable regulation of both average radiance and spectrum to match the spectral radiance of at least three simulated types of solar backgrounds.

It is technically difficult to develop a broadband UV-NIR light source of variable light intensity and variable spectrum capable to be fitted to the three simulated solar backgrounds described in section 4. The spectrum of the simulated solar backgrounds is not similar to the spectrum of xenon lamps commonly used in solar illuminators (Fig. 12). In detail, the spectrum of the xenon lamp can be considered similar to the spectrum of the concrete/snow background in the band from about 400 nm to 800 nm, but there are large differences for wavelengths below 350 nm. In the case of the sky background, the differences are large in the entire analysed spectral range.

None of the commonly available optical filters match the spectrum of common UV-NIR light sources with the spectrum of simulated solar backgrounds. The task is difficult even when using a filter combination. At the same time, it should be remembered that number of simulated backgrounds will significantly increase if the task of the test system is to increase from simulating only worst-case scenarios to simulating both worst-case and average work scenarios. Practically, it means that even an almost perfect broadband light source of a three step regulation of spectral radiance and capable of simulating three interesting types of solar backgrounds (sky background, concrete background, snow background) can be found an unsatisfactory solution by the most demanding test teams.

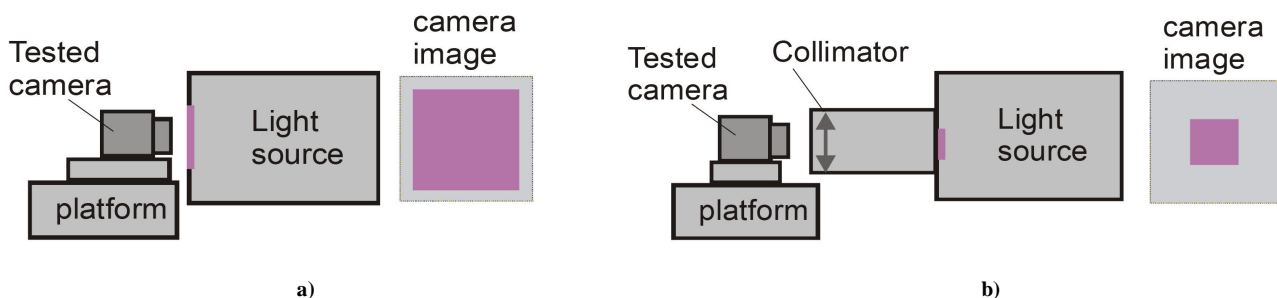


Fig. 11. Tests of solar sensitivity: a) light source fills FOV of the tested SBUV camera, b) SBUV camera sees the simulated solar background as part of its FOV.

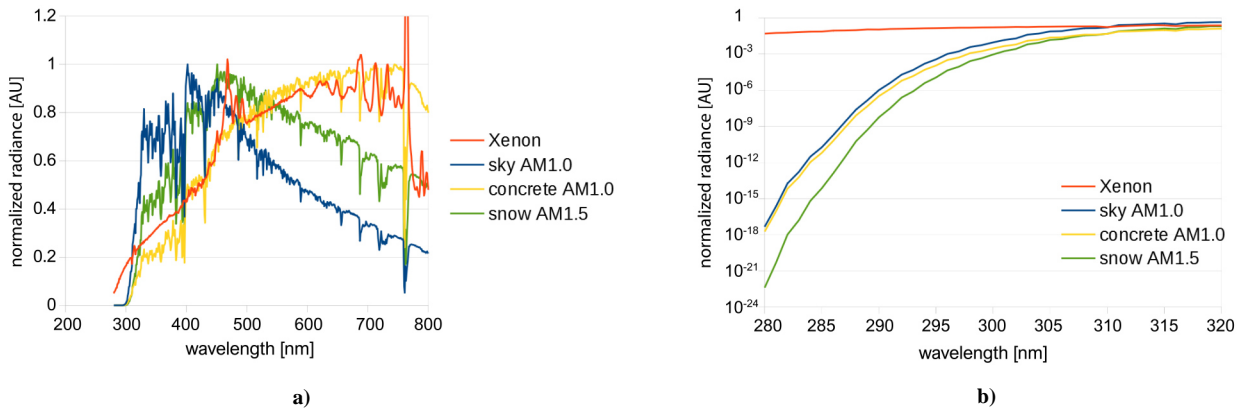


Fig. 12. Comparison of the typical relative spectrum of a typical xenon lamp with the spectrum of a solar background to be simulated: a) linear scale, b) logarithmic scale.

In such a situation a more universal technical solution is proposed. This universal solution is based on a concept of an image projector that can work in two modes: 1) broadband mode, 2) multi-band mode (a series of exchangeable narrow bands). In the broadband mode, the spectrum of the light source is nearly identical with the spectrum of simulated backgrounds only in a critical narrow band where the solar edge drop is located (from about 280 nm to about 310 nm) and the spectrum of SBUV cameras typically overlays the solar spectrum. A significant difference between the source spectral radiance and the background spectral radiance is acceptable in the spectral band from the simulated solar edge to the limit of sensitivity of UV image intensifiers (typically about 800 nm). The latter spectral band can be sampled when the light source works in a multi-band mode.

The proposed image projector has been built according to the design concept shown in Fig. 13. The xenon bulb is used as the original light source. The light beam emitted by the xenon bulb is focused by the condenser lens at the entrance to the light integrator block. This block creates a light emitting uniform disk at its output due to multiple

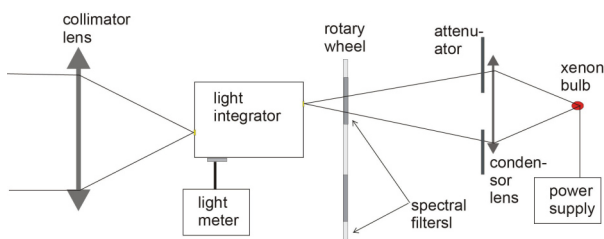


Fig. 13. Simplified diagram of an image projector for the solar testing of SBUV cameras.



Fig. 14. Photo of the USOL system built according to the design concept shown in Fig. 13.

reflections. Later, the image of the light emitting disk at the light integrator output is projected by the collimator towards the tested SBUV camera.

This design concept has been used by authors to build a system for solar tests of the SBUV cameras (coded as USOL system) shown in Fig. 14. Main technical parameters of the USOL station are shown in Table 2.

As can be seen in Fig. 15, the spectrum of light emitted by USOL station working in a broadband mode is almost identical to the spectrum of the solar backgrounds to be simulated only in a narrow spectral band, where the solar spectral edge is located between 280 and 320 nm. It differs significantly from the spectrum of solar backgrounds in the full spectral band of 280–800 nm that is to be analysed. Therefore, measuring the solar sensitivity of SBUV

Table 2.
Main specifications of the USOL test station.

Parameter	Value
Angular size of the projected image of the light source	Circular 2°
Modes of work	1) broadband, 2) multi-band
Broadband mode:	
Calibrated spectral band	From simulated solar edge to 800 nm
Number of simulated reference solar backgrounds	Three: 1) sky AM1.0, 2) concrete AM1.0, 3) snow AM1.5 (option: the number can be increased)
Light spectrum of reference backgrounds	As shown in Fig. 15
Range of regulated luminance	150–150 000 cd/m ²
Regulation resolution	Not worse than 1.00%
Multi-band mode:	
Number of simulated spectral bands	Ten: < 320 nm, 320–350 nm, 350–385 nm, 385–420 nm, 420–485 nm, 485–550 nm, 550–630 nm, 630–695 nm, 695–780 nm, >780 nm
Regulation dynamics of light intensity in any of these spectral bands	At least 1000 times

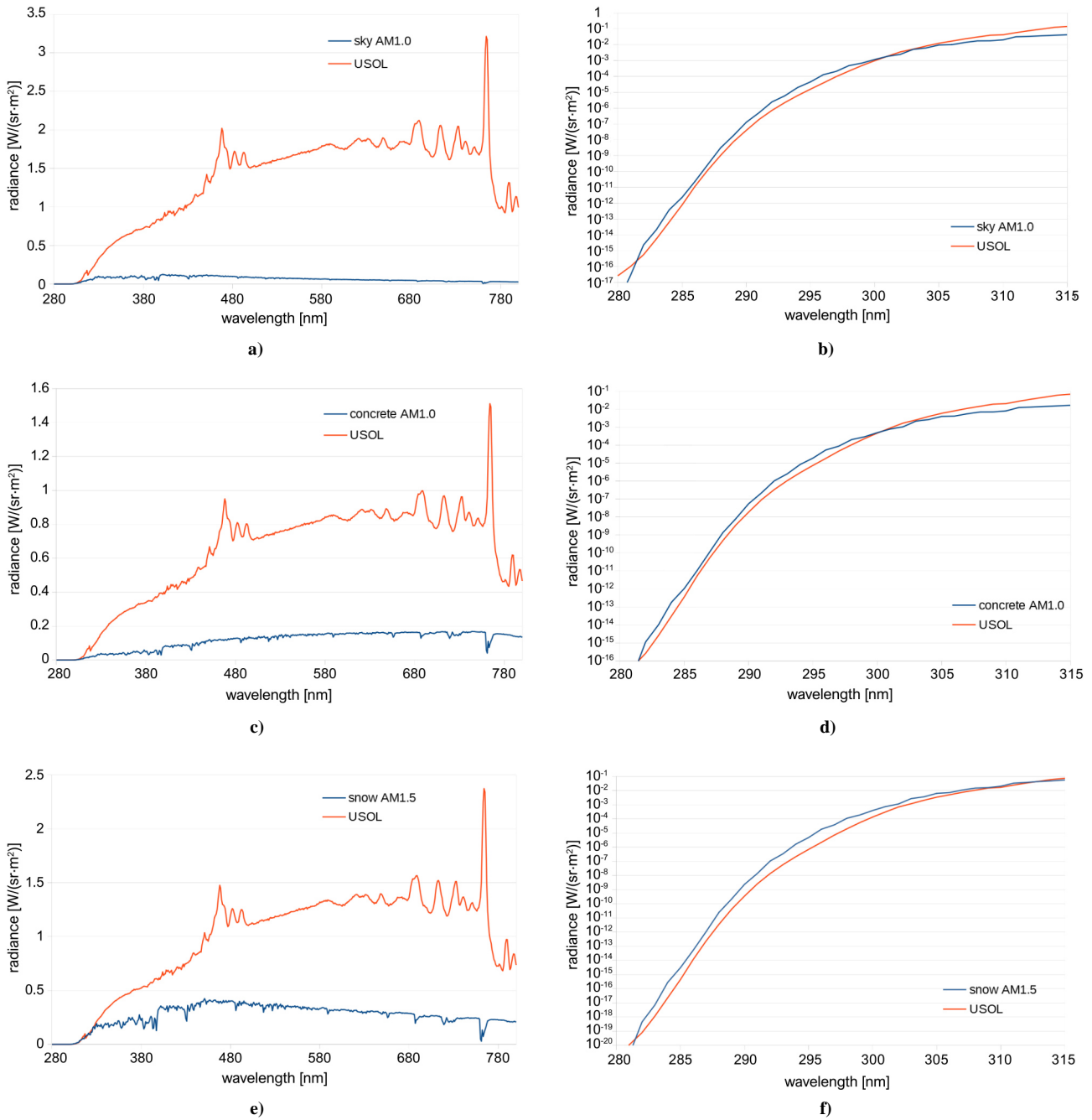


Fig. 15. Comparison of the spectrum of USOL station in broadband mode with the spectrum of solar backgrounds to be simulated: a, b) summer sky background at AM1.0; c, d) summer concrete background at AM1.0; e, f) spring snow at AM1.5.

cameras using the USOL station working in any of the broadband sub-modes will generate inaccurate results.

In order to enable the accurate measurement of the solar sensitivity of SBUV cameras for the three analysed reference solar backgrounds (and possibly other solar backgrounds met in the real work of SBUV cameras), the following measurement algorithm has been proposed:

1. Switching of USOL station to simulate the appropriate type of the solar spectral edge (AM1.0 or AM1.5) in a spectral band of 280–320 nm suitable for the simulated background.
2. Regulation of radiance L_{USOL} of the image projected by the USOL station working in a broadband mode to the level in which the projected image generates an output signal in the linear range of the tested

SBUV camera. Practically, it means that the output signal from the projected solar image to the output signal from the internal noise is not higher than about 5 times.

3. Measurement of the raw solar sensitivity ($SolarS_{raw}$) understood as the ratio of the average output signal (spatio-temporal density of even counts) at the output of SBUV camera generated by the USOL station to the average output signal generated by the camera internal noise.
4. Switching of USOL station to work in a multi-band mode.
5. Measurement of the relative uncorrected spectral responsivity $SpecR_{raw}$ of the SBUV camera on a set of discrete spectral bands. This measurement is

done by comparing the output signals recorded in different n spectral bands.

6. Correction of the measured $SpecR_{raw}(i)$ by taking into account the width and transmission of the n spectral bands and the spectral radiance of the light source in a broadband mode. New $SpecR_{cor}$ is calculated.
7. Calculation of the corrected solar sensitivity ($SolarS_{cor}$):

$$SolarS_{cor} = SolarS_{raw} / \frac{\sum \frac{L_{real}(i)}{L_{ref}(i)} \cdot SpecR_{cor}(i)}{\sum SpecR_{cor}(i)}, \quad (6)$$

where i is the number of the spectral band, $SpecR_{cor}(i)$ is the corrected spectral sensitivity of the SBUV camera in i spectral band, $L_{ref}(i)$ is the average spectral radiance of the simulated solar background in i spectral band, and $L_{real}(i)$ is the radiance of the image projected by the test station.

It should be noted that the proposed solution of the test station is capable to work in two work modes (broadband and multi-band) and offers not only ability to measure sensitivity to practically any solar backgrounds, but also to determine wavelengths in which there is overlapping of spectral sensitivity of the tested SBUV camera and spectral radiance of the analysed solar background. The latter option is particularly useful for SBUV cameras manufacturers because it enables a design optimization for a specific geographical region.

8. Practical tests

The method of verifying the proposed measurement concept of solar sensitivity of the SBUV cameras seems apparently easy. It is necessary to compare the measurement results of solar sensitivity measured in the field conditions when FOV of the tested SBUV camera is at least partially filled by one of reference solar backgrounds with the results obtained under laboratory conditions, when the test station simulates the same solar background. The test concept could be considered experimentally verified if the measurement results of solar sensitivity obtained in the field tests are similar to the results obtained in the solar laboratory tests.

In practice, it is difficult to carry out a proper experimental verification of the proposed concept of the measurement sensitivity of SBUV cameras to solar light due to three requirements for such tests:

1. The test should be carried out using a series of SBUV cameras from different manufacturers (preferable have all cameras for all field tests). This

requirement practically means the high cost of the potential purchase of a long series of SBUV cameras for testing because temporary free leasing is almost impossible due to the distrust of the manufactures about consequences of such tests for the marketing of their cameras.

2. Tests should be performed for at least three types of reference solar backgrounds: solar, concrete, snow with the required AM coefficient. This requirement is relatively easy to fulfil but some travel is needed to locations where the required backgrounds can be found. It should be noted that timely travel is needed to find the snow background.
3. Tests should be performed at a number of geographical locations in the mid-latitude zone in order to calculate average values for the measured solar sensitivity. In this case extensive travels are needed to increase test results reliability.

The authors of this paper cannot fulfil requirements for such ideal field tests for several reasons:

1. The authors do not have funds to purchase a dozen of needed SBUV cameras. They managed to rent only two SBUV cameras directly from one of the manufacturers and two second-hand SBUV cameras from users of such cameras in the electric power industry.
2. Very limited information is available on solar sensitivity of the rented SBUV cameras: the suppliers know only which camera performs better in summer conditions.
3. The USOL test station has become fully operational since the beginning of November 2020. Autumn, winter and early spring are not good times for testing solar sensitivity of the SBUV cameras in the authors' geographical location (Poland, Europe). It is necessary to wait at least about 6–7 months to have proper illumination conditions (AM below 1.5).
4. The authors do not have funds and time for extensive travels needed for proper field tests.
5. Going abroad is not possible nowadays due to the Covid-19 pandemic restrictions.

The aforementioned factors mean that the proper experimental verification of the proposed test concept will not be done in the near future. In such a situation, the authors of this paper decided to carry out only a limited experimental verification of the proposed test concept and limit the purpose to checking if the tests performed using the USOL station can properly indicate two cameras that are considered the best ones by the suppliers of two pairs of SBUV cameras. The results of such preliminary limited tests are shown in Table 3. Value <1 means that the tested camera is not sensitive to the simulated solar background.

Table 3.

Results of the preliminary experimental tests of the proposed solar test concept (<1 camera is resistant to the simulated spectrum).

Camera code	Camera age	Supplier opinion	$SolarS$ (sky AM1.0)	$SolarS$ (concrete AM1.0)	$SolarS$ (snow AM1.5)
A	Used	Better	4.1	2.3	<1
B	Used	Worse	16.5	5.2	<1
C	New	Better	<1	<1	<1
D	New	Worse	1.5	<1	<1

A number of conclusions can be drawn based on the data in Table 3.

First, SBUV cameras offered on the market differ significantly in terms of protection against solar light. There are cameras totally or almost totally insensitive to even the most extreme natural solar backgrounds and cameras that cannot make any useful measurement under extreme solar conditions (simulated AM1.0).

Second, all tested SBUV cameras passed the AM1.5 snow sensitivity test in the solar background. No measurable sensitivity to such a solar background was detected. Such results suggest that the leakage range of the cameras A and B is in the spectral band of 280–320 nm where there is a large difference between AM1.0 background and AM1.5 background.

Third, there is a good agreement between the measured solar sensitivity and the opinion of the tested SBUV cameras owners on the cameras sensitivity to solar light. Worse sensitivity values correlate adequately with cameras that were considered worse.

9. Conclusions

Sensitivity of the SBUV cameras to solar light emitted/reflected by backgrounds of corona targets is one of the crucial parameters describing the performance of such cameras under day light conditions. Despite its importance, the problem of determining the solar sensitivity of SBUV cameras has not been analysed and solved in specialized literature, so far. This paper presents the concept (definition, measurement method, test equipment, test results) for measuring solar sensitivity of SBUV cameras.

Preliminary experimental test confirmed that the test station built using the proposed test concept can correctly indicate SBUV cameras that perform better in summer light conditions. However, the scope of the experimental tests has been significantly limited and further extended field tests are needed to fully validate the proposed concept of the SBUV cameras solar testing.

Authors' statement

Research concept and design, K Chrzanowski; collection and/or assembly of data, B. Stafiej and K. Chrzanowski; data analysis and interpretation, K. Chrzanowski and B. Stafiej; writing the article, K. Chrzanowski; critical revision of the article, B. Stafiej; final approval of the article, K. Chrzanowski. and B. Stafiej.

References

- [1] UVIRCO Technologies. <https://www.uvirco.com> (2020).
- [2] OFIL Systems - Daytime Corona Cameras. <https://www.ofilsystems.com> (2020).
- [3] Zhejiang ULIRVISION Technology Co., LTD. <https://www.ulirvision.co.uk> (2020).
- [4] Olip Systems Inc. <https://www.olipsystems.com> (2020).
- [5] Sonel S.A. - Przyrządy pomiarowe, kamery termowizyjne. <https://www.sonel.pl> (2020).
- [6] ICI Infrared Cameras Inc. <https://www.infraredcameras.com> (2020).
- [7] Chrzanowski, K. & Chrzanowski, W. Analysis of a blackbody irradiance method of measurement of solar blind UV cameras' sensitivity. *Opto-Electron. Rev.* **27**, 378–384 (2019). <https://doi.org/10.1016/j.opelre.2019.11.009>
- [8] Cheng, H. et al. Performance characteristics of solar blind UV image intensifier tube. in *Proc. SPIE – International Symposium on Photoelectronic Detection and Imaging 2009: Advances in Imaging Detectors and Applications* **7384** (2009). <https://doi.org/10.1117/12.834700>
- [9] Coetzer, C., West, N., Swart, A. & van Tonder, A. An investigation into an appropriate optical calibration source for a corona camera. in *IEEE International SAUPEC/RobMech/PRASA Conference* 1–5 (2020). <https://doi.org/10.1109/saupec/robmech/prasa48453.2020.9041014>
- [10] Coetzer, C. et al. Status quo and aspects to consider with ultraviolet optical versus high voltage energy relation investigations. in *Proc. SPIE – Fifth Conference on Sensors, MEMS, and Electro-Optic Systems* **11043**, 1104317 (2019). <https://doi.org/10.1117/12.2501251>
- [11] Du Toit, N.S. Calibration of UV-sensitive camera for corona detection. (Stellenbosch University, South Africa, 2007). <http://hdl.handle.net/10019.1/2920>
- [12] Pissulla, D. et al. Comparison of atmospheric spectral radiance measurements from five independently calibrated systems. *Photochem. Photobiol. Sci.* **8**, 516–527 (2009). <https://doi.org/10.1039/b817018e>
- [13] Clack, C. T. M. Modeling solar irradiance and solar PV power output to create a resource assessment using linear multiple multivariate regression. *J. Appl. Meteorol. Climatol.* **56**, 109–125 (2017). <https://doi.org/10.1175/JAMC-D-16-0175.1>
- [14] G03 Committee. Tables for Reference Solar Spectral Irradiances: Direct Normal and Hemispherical on 37 Tilted Surface. <http://www.astm.org/cgi-bin/resolver.cgi?G173-03R20> <https://doi.org/10.1520/G0173-03R20>
- [15] Tohsing, K., Klomkliang, W., Masiri, I. & Janjai, S. An investigation of sky radiance from the measurement at a tropical site. in *AIP Conference Proceedings* **1810**, 080006 (2017). <https://doi.org/10.1063/1.4975537>
- [16] Chen, H.-W. & Cheng, K.-S. A conceptual model of surface reflectance estimation for satellite remote sensing images using in situ reference data. *Remote Sens.* **4**, 934–949 (2012). <https://doi.org/10.3390/rs4040934>
- [17] Gueymard, C. A. Parameterized transmittance model for direct beam and circumsolar spectral irradiance. *Sol. Energy* **71**, 325–346 (2001). [https://doi.org/10.1016/S0038-092X\(01\)00054-8](https://doi.org/10.1016/S0038-092X(01)00054-8)
- [18] Gueymard, C. *SMARTS2: a simple model of the atmospheric radiative transfer of sunshine: algorithms and performance assessment. Professional Paper FSEC-PF-270-95.* (Florida Solar Energy Center, 1995).
- [19] Gueymard, C. A. Reference solar spectra: Their evolution, standardization issues, and comparison to recent measurements. *Adv. Space Res.* **37**, 323–340 (2006). <https://doi.org/10.1016/j.asr.2005.03.104>
- [20] TOMS Meteor-3 Total Ozone UV-Reflectivity Daily L3 Global 1 deg x 1.25 deg V008, Greenbelt, MD, Goddard Earth Sciences Data and Information Services Center (GES DISC), *TOMS Science Team*, https://disc.gsfc.nasa.gov/datacollection/TOMSM3L3_008.html (2021).
- [21] SMARTS: Simple Model of the Atmospheric Radiative Transfer of Sunshine. *National Renewable Energy Laboratory*. <https://www.nrel.gov/grid/solar-resource/smarts.html> (2020).
- [22] Cooper, O. R. et al. Global distribution and trends of tropospheric ozone: An observation-based review. *Elem. Sci. Anth.* **2**, 000029 (2014). <https://doi.org/10.12952/journal.elementa.000029>
- [23] Riordan, C. & Hulstron, R. What is an air mass 1.5 spectrum? (solar cell performance calculations). in *IEEE Conference on Photovoltaic Specialists* (1990). <https://doi.org/10.1109/pvsc.1990.111784>
- [24] Wikipedia contributors. Air mass (solar energy). *Wikipedia*. [https://en.wikipedia.org/wiki/Air_mass_\(solar_energy\)](https://en.wikipedia.org/wiki/Air_mass_(solar_energy)) (2020).
- [25] Ritter, M. E. The Physical Environment: an Introduction to Physical Geography. <https://www.thephysicalenvironment.com> (2020).
- [26] NOAA Research. NOAA Solar Position Calculator. <https://www.esrl.noaa.gov/gmd/grad/solcalc/azel.html> (2020).
- [27] Solargis. Global Solar Atlas. <https://globalsolaratlas.info/download/world> (2020)

- [28] Blanc, P. *et al.* Direct normal irradiance related definitions and applications: The circumsolar issue. *Sol. Energy* **110**, 561–577 (2014). <https://doi.org/10.1016/j.solener.2014.10.001>
- [29] Class ABB Small Area Solar Simulators. *Newport Corporation*. <https://www.newport.com/f/small-area-solar-simulators> (2020).
- [30] Dai, C., Wu, Z., Qi, X., Ye, J. & Chen, B. Traceability of spectroradiometric measurements of multiport UV solar simulators. in *Proc. SPIE - International Symposium on Photoelectronic Detection and Imaging 2013: Imaging Spectrometer Technologies and Applications* **8910**, 8910-2 (2013). <https://doi.org/10.1117/12.2030753>
- [31] Christiaens, F. & Uhlmann, B. *Guidelines for Monitoring UV Radiation Sources*. (COLIPA, 2007).
- [32] Qualitätsmanagement-Handbuch, Abteilung 7, Physikalisch-Technische Bundesanstalt (PTB), https://www.ptb.de/cms/fileadmin/internet/fachabteilungen/abteilung_7/QMH_Abt7_KAP3_1_A16_a.pdf (2020). [in German]